ISSN 1330-3651 (Print), ISSN 1848-6339 (Online)
https://doi.org/10.17559/TV-20250207002344
Original scientific paper

Design and Analysis of a Novel Non-isolated DC-DC MMC Architecture for HVDC Power Networks Interconnections

Abdurrahim ERAT*, Ahmet Mete VURAL

Abstract: High voltage direct current (HVDC) power structures provide various notable advantages over high voltage alternating current (HVAC) power grid structures, including superior efficiency, faraway and large-scale transmission power, flexibility, controllability, minimal operating costs with positive effects on the environment, interconnection of asynchronous power systems. As HVDC systems are implemented, the demand for advanced DC-DC converters to facilitate voltage-level adaptations in interconnected networks has grown. The DC-DC Modular Multi-level Converters (MMCs) are a tremendously practical and cost-effective converter architecture appealing for interconnecting HVDC power systems. This study presents a unique DC-DC MMC architecture that provides an excellent solution for integrating modern asynchronous HVDC networks and these modern HVDC power systems with existing HVAC power systems. The suggested innovative DC-DC MMC has numerous advantages, including lower volume, more appealing funding cost, and less SMs quantity. The transformerless approach significantly reduces the converter's volume, weight, price, and power loss. To precisely control the power transfer among power systems with varying or comparable voltage levels, this unique study presents a power transfer control system. The performance of the proposed system is validated through mathematical modelling, harmonic analysis, and simulations, demonstrating its capability to effectively interconnect HVDC power systems.

Keywords: DC-DC MMC; DC-DC power conversion; HVDC; Interconnection of asynchronous power grids; MMC

1 INTRODUCTION

Recently, there has been a significant increase in infrastructure for producing power utilizing renewable energy sources for stable power systems due to the risk of depletion and harmful environmental impacts of traditional energy sources [1, 2]. Renewable energy sources-based power systems have developed dramatically due to the substantial growth in energy demands, which are essential to the survival of humanity, and the demand for more effective energy generation, transmission, and distribution. On the other hand, renewable energy-based power plants, such as solar and wind, are often located relatively far away from load centres [3]. Specifically, offshore wind-powered power plants are situated far from the mainland. HVDC technology is crucial when sending electrical power generated far from the mainland to load centres over tremendous distances or offshore [4-6]. HVDC technology is essential to today's power systems because of characteristics including adaptability, efficiency in power transmission, affordable and technical advantages, eco-friendly, narrow transmission line losses, appropriate for high power large-scale, high-power transmission throughout extensive distances, combining asynchronous power systems, submarine cable connection, defence to deviations in phase angle, frequency, impedance, or voltage, sustaining standalone frequency and generator management especially when compared to conventional HVAC power systems [4, 5, 7, 8]. The fundamental HVDC technology architecture is depicted in Fig. 1.

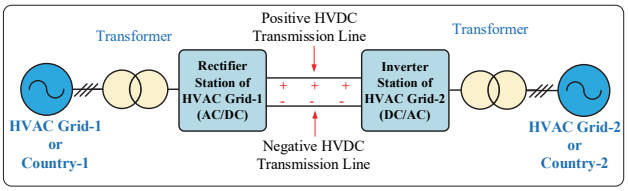

Figure 1 The fundamental architecture of HVDC technology

It is clear from the characteristics mentioned above that HVDC technology will play a crucial role in the power networks of the present-day power networks of the coming decades. HVDC technology is significant in today's power systems, overwhelmingly due to power electronics-based converter technologies. Put another way, the fast advancement of semiconductor-based power electronics technology has made it possible for HVDC technology to be a significant component of modern power systems. The converter units located at the connection points of HVDC technology are frequently centred on voltage source converters (VSC) or line commutated converters (LCC) [9]. Furthermore, multi-level converter technologies have lately been essential to HVDC power applications.

At the same time, LCC-based HVDC (LCC-HVDC) and VSC-based HVDC (VSC-HVDC) systems have historically been employed in various HVDC power technologies. Fig. 2 and Fig. 3 demonstrate the HVDC structure based on an LLC (CSC) and a VSC, respectively.

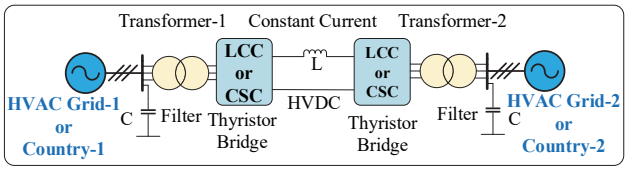

Figure 2 LCC or CSC-based HVDC power structure

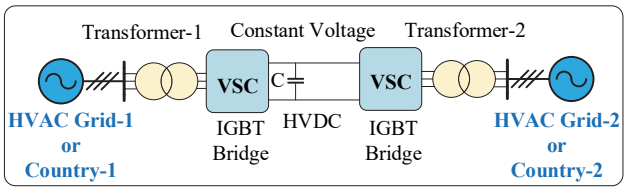

Figure 3 VSC-based HVDC power structure

More substantial capacity and higher voltages are required for significant power transmission in HVDC electrical power systems. In general, the voltage transportation, the degree of harmonics, and the individual component stress of power converters are the main obstacles to the widespread and effective utilization of the successive linking approach for powering instruments to

boost efficiency in typical HVDC power systems. Power system researchers have created several novel multi-level structures for HVDC power systems or modular integrating techniques. Due to recent improvements in semiconductor-based power electronics technology, multi-level converter systems will primarily be utilized in HVDC technology. From an alternative viewpoint, multi-level converter systems have progressively gained prominence in recent years, employing HVDC power technology in conjunction with conventional DC-DC converter topologies. Specifically, as a consequence of having power quality enhancement, reliability, high efficiency, lower power switch rating, excellent output capacity, substantial modularity, straightforward scaling, transformerless operating capabilities, tolerant of failures, utilizing typical elements, extremely readily accessible, and straightforward operation system [9-12] valuable characteristics, MMC [13, 14] technology which is a multi-level structure has attracted the interest of a large number of researchers studying HVDC power systems applications. Power electronics-based DC-DC converter designs have undoubtedly played a significant role in the recent fast development of HVDC technologies.

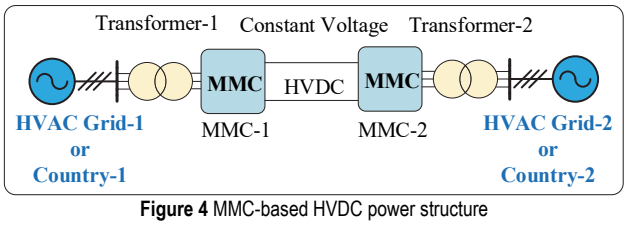

Figure 4 MMC-based HVDC power structure

Nevertheless, the recent introduction of MMC technology has contributed significantly to the tremendous momentum that HVDC technology has received. Day by day, the share of MMC-based HVDC technologies in power systems grows dramatically. The MMC-based HVDC structure is illustrated in Fig. 4. In power systems, conventional MMC technology established in the literature can be implemented as an inverter station (DC-AC) and a rectifier station (AC-DC). MMC technology is efficiently employed in numerous applications, including HVDC power transmission systems [15], static synchronous compensator (STATCOM) utilizations [16], DC-DC transformation systems [17], battery energy storage systems [18], developing electric ships [19], variable-speed drives for motors [20], active power filters [21], electric vehicles [22], solar photovoltaic systems [23], because of its beneficial advantages.

Due to its increasing popularity, DC-DC MMC technology, accomplished through utilizing conventional MMC technology as a reference, has drawn the curiosity of many researchers. In DC-DC MMC topologies, some topologies are isolated by a transformer between the primary and secondary sections of the designs. In non-isolated topologies, no transformer is used between the primary and secondary sections of designs. DC-DC MMC technology provides excellent results, particularly in integrating modern asynchronous HVDC power systems and new-generation HVDC power systems with existing asynchronous HVAC power systems. Many DC-DC MMC layouts have been developed for HVDC power system interconnections based on classical MMC technology. In particular, DC-DCMMC configurations are vital in interconnecting multi-level HVDC power systems with various voltage levels. Numerous DC-DC MMC topologies have been published in the literature due to their adaptable and modular architecture. Tab. 1 presents the notable achievements and novel characteristics associated with several DC-DC MMC topologies identified in the literature. In cases where it comes to combining HVDC power networks with different voltage levels and incorporating them with already-existing asynchronous HVAC power networks, DC-DC MMC technology is critically important. The preceding scenario is substantially supported by Tab. 1, and multiple noteworthy DC-DC MMC configurations discovered in the literature are nevertheless included in Tab. 1.

A unique DC-DC MMC design is introduced in this study to integrate two asynchronous HVDC power grids successfully. The operation of the fundamental nature, simulation-based parameter records, and mathematical analysis of the relevant topology have all been thoroughly analysed. This study offers a novel DC-DC MMC design essential to fulfilling the demands of HVDC technology, which is gaining popularity among power system researchers and entrepreneurs daily. It provides an excellent approach to integrating modern HVDC power networks with varying voltage levels, which are increasingly used in power systems. Connecting contemporary HVDC power systems with existing HVAC power networks is crucial. A rectifier station is used in the proposed DC-DC MMC system to effectively merge two asynchronous HVAC networks. The voltages of the two HVAC networks are transferred to the primary and secondary sides of the suggested DC-DC MMC system after being rectified and controlled in these rectifier stations. A general control approach has been used in this study for both the DC-DC MMC design and the HVAC power networks, even though MMC-based control techniques are often advised in similar AC-DC, DC-AC, AC-AC, and DC-DC MMC configurations. The phase-locked loop (PLL) block and reference values are utilized to transfer the network data of the two HVAC power networks to the voltage, current, and power control units after they have been through a filter system. The Proportional-Integral-Derivative (PID) technology used in these units facilitates the acquisition of the best possible data for DC-DC MMC systems and networks.

A satisfactory power transfer was observed, considering the suggested arrangement was implemented in a simulated environment based on the simulation outcomes. The fourth section of the research goes into detail about the control system. Therefore, the suggested DC-DC MMC topology offers several improvements, novelties, and noteworthy achievements compared to the existing DC-DC MMC topologies in the literature, many of which are based on the previously stated facts. First, the suggested DC-DC MMC architecture is created as an entirely novel topology. Second, the structure of the proposed topology is symmetrical and remarkably modular. Third, bidirectional power transfer is effectively achieved since it is created in a symmetrical arrangement. Fourth, its primary and secondary power grids can receive regular currents via the proposed design. Fifth, the transformerless approach significantly reduces the

converter's volume, weight, cost, and power losses. Sixth, the adaptable and modular architecture of the suggested innovative converter design with various sets of SMs groups substantially enhances its capacity for transforming electrical power while combining asynchronous power networks. Seventh, an extensive voltage rating variety and flexible performance between power networks are made possible by the innovative architecture. Eighth, it successfully integrates modern asynchronous HVDC power networks and can incorporate modern HVDC power networks with existing asynchronous HVAC power networks. Ninth, the modular architecture ensures scalability at high voltage levels, enhancing power network integration. The tenth, the employed control strategy, provides prompt and efficient power transfer between interconnected HVDC power grids.

Table 1 Some DC-DC MMC topologies' contributions to the literature and application areas.

DC-DC MMC Study	Application Area	Contribution to Literature
[9]	Hybrid HVDC grid interconnections	The suggested concept can connect HVDC networks utilizing VSC and LCC and operate in four quadrants.
[24]	MVDC grids	The study presents a bipolar MMDC operational approach to achieve stable performance in bipolar MVDC power distribution networks.
[25]	HVDC grids	The suggested arrangement using the fewest possible semiconductors can effectively deliver high DC voltage multiplication through a DC failure- avoiding ability and sustained bi-directional power transmission.
[26]	HVDC grid interconnections	The suggested design has several benefits, including a reduced volume, more appealing investment costs, and reduced submodules (SMs).
[27]	Rapid charging of electric vehicles	The suggested design reduces the control complexities and switching numbers using a single half bridge-MMC arm. It can naturally prevent DC faults, and a high voltage conversion rate can be obtained through galvanic isolation.
[28]	LVDC and MVDC grid interconnections	Decreased computational stress for power enforcement, circulating current mitigation, DC fault ride-through functioning, and transformer current optimization for improved effectiveness throughout the whole load range have been made possible by the suggested design.
[29]	MVDC and HVDC grid interconnections.	This paper suggests using magnetizing inductance as a basis for an analytic analysis of the DC-DC MMC's performance. The difference method circulating current, converter powers, currents, capacitor voltage ripples, and soft-switching behavior are all shown to be significantly impacted by the magnetizing inductance.
[30]	LVDC and HVDC grid interconnections.	The primary benefit of the suggested converter is that it utilizes a single bidirectional high-voltage valve and traditional MMC arms with half bridge SMs (HBSMs) to achieve DC-DC transformation alongside appropriate capacitor voltages and restricted voltage ripples.
[31]	MV DC-DC interconnections	Compared to the MMC, the suggested design requires just one-third of the SMs, voltage, and current sensors to produce three-phase trapezoid outputs with a regulated sloping. The DC fault-blocking capacity, flexible grounding, and desirable voltage matching are all provided by the front-to-front arrangement of the suggested design.
[32]	DC distribution grids	In contrast to the conventional MMC, the suggested design allows the buck cell to produce smoother voltage control and a larger voltage band. The excellent efficiency of the MMC-based DAB unit is ensured by the assured voltage corresponding between the LV and MV ends over the whole voltage band.
[Proposed Study]	HVDC power grid interconnections	This study presents a unique DC-DC MMC architecture that provides an excellent solution for integrating modern asynchronous HVDC networks and these modern HVDC power systems with existing HVAC power systems. The transformerless approach significantly reduces the converter's volume, weight, price, and power loss. The suggested converter exhibits several characteristics, including a straightforward circuit design, innovative structure, acceptable swift dynamic reaction, controllability, and bidirectional power flow. A power transfer control system is presented in this unique study to accurately regulate the power transfer across power systems with different or similar voltage levels.

The safety issue in the proposed non-isolated DC-DC MMC topology is solved with a completely and perfectly compact structure, symmetrical characteristics, individualized grounding at each station, and a functional control mechanism that protects the system in case of possible faults. In other words, the symmetrical, modular, and compact structure of the DC-DC MMC design that is being shown demonstrates a protective and safe characteristic in the integration of power networks. Every arm and every set of SM (HBSM) in every arm was viewed as an individual compact structure throughout the design stage. This compact structure eliminates potential safety concerns. The modular and compact design approach increases the system's redundancy, guaranteeing that the system remains functional regardless of whether a module fails. A framework such as this additionally facilitates maintenance and repair procedures more straightforwardly. Each component's nominal operating voltage and current in the suggested converter design have been carefully specified to exceed the expected maximum ratings by a significant margin to reduce the risk of system failures. Potential safety concerns are minimized given that the system's control mechanism has been designed to react rapidly to faults, maintain system stability, recognize abnormal situations, and give preventive actions. Protective grounding mechanisms also guarantee trouble-free operation in HVAC and HVDC power grid stations. These safeguards ensure that power transmission occurs appropriately in the suggested topology and the overall power system.

2 MMC TECHNOLOGY

The conventional MMC topology, initially put forward in a German patent by Prof. Marquardt in 2001 [13], is illustrated in Fig. 5. The patent, as mentioned earlier, illustrates the inductances within each arm, the half-bridge (HB) and full-bridge) FB) submodules (SMs), and the DC to three-phase converter structure, including a sequence of interconnected SMs. Regarding many applications, the

conventional MMC architecture can function either as a rectifier (AC-DC) or as an inverter (DC-AC). Each phase in the traditional MMC design comprises the upper and lower arms, as seen in Fig. 5. An arm inductor (*L*, *r*) and HB or FB SMs connected in series constitute each upper and lower arm. A branch leg originates from each phase's midpoints (*a*, *b*, and *c*) and connects the system's three-phase AC terminals (*Va*, *Vb*, and *Vc*) via a phase inductor (*Lo*, *ro*). In other words, the design's AC terminal is linked to the centre of every phase; meanwhile, the DC terminal is connected between the upper and lower arms of the phases. The appropriate AC and DC currents are produced by the regulated voltages every single arm produces at individual endpoints in conjunction with the appropriate DC and AC design voltages.

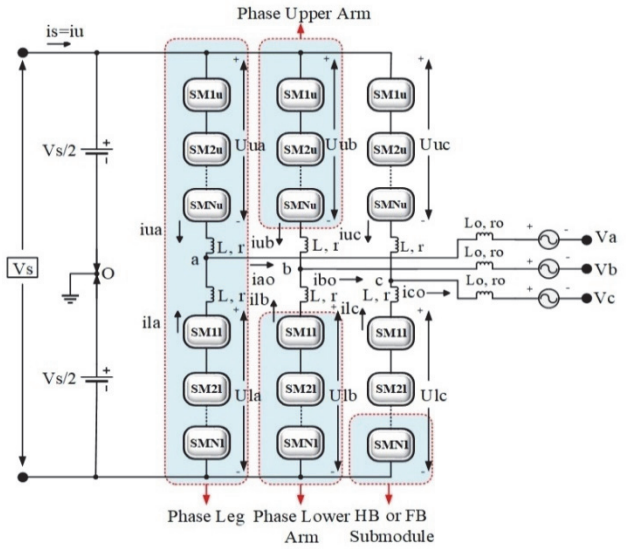

Figure 5 The classical MMC structure

The SM structure is critical in multi-level converter topologies, especially in MMC concepts. From the time the MMC structure was initially presented in the literature until today, multiple SM topologies have been developed by many researchers. As demonstrated in Fig. 6, SM structures can be categorized into two main groups according to the output voltage level: single-source two-level SM topologies and multiple-source multi-level SM topologies [33]. Undoubtedly, one of the primary explanations for the recent increase in curiosity regarding MMC technology is the significant advancements in semiconductor technology.

Given that SM structures, which are the backbone of MMC technology, consist of semiconductor-based power switching elements, they are due to their outstanding characteristics, including their capacity to operate at more substantial temperatures and reduced switching losses. High switching capabilities, Metal-Oxide-Semiconductor Field-Effect Transistors (MOSFETs), and insulated gate bipolar transistors (IGBTs) power-switching components based on silicon carbide and gallium nitride are utilized in SM architectures of MMC designs. HB topology is a unipolar semiconductor-based circuit structure most frequently used in SM circuits because of its straightforward construction. HBSM has lesser power losses because of its straightforward structure. The FBSM structure is a semi-conductor-based circuit construction that consists of one floating capacitor and two HBSMs. The FBSM structure provides effective defences against DC fault currents. However, there are more considerable power losses because there are more semiconductor-based power-switching devices than in the HBSM structure [18]. Fig. 7 illustrates the SM structures researchers most frequently utilize in MMC architectures. IGBT-based HBSM and FBSM architectures are depicted in Fig. 7a and Fig. 7b correspondingly. The MOSFET-based HBSM form is illustrated in Fig. 7c, while the MOSFET-based FBSM architecture is presented in Fig. 7d.

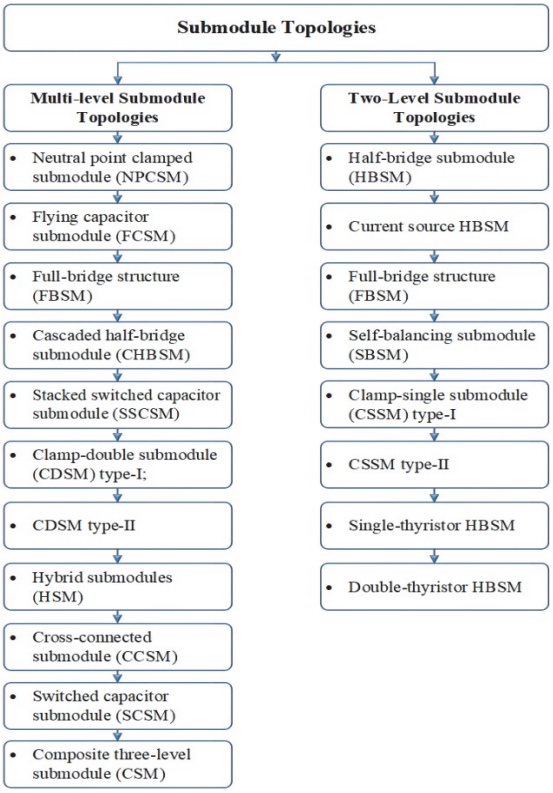

Figure 6 SM architectures utilized in MMC designs

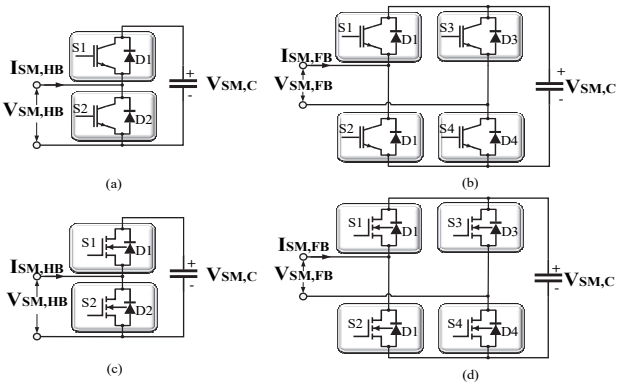

Figure 7 The SM structures most frequently utilized in MMC designs: (a) IGBT-founded HBSM; (b) IGBT-founded FBSM; (c) MOSFET-founded HBSM; (d) MOSFET-founded FBSM

3 PROPOSED NON-ISOLATED DC-DC MMC MODEL

HVDC technology has recently played a more significant role in global power networks. Nonetheless, it is unavoidable that some integration issues exist between new-generation HVDC power systems with various voltage levels and conventional HVDC power systems.

Simultaneously, combining HVDC power networks with HVAC power networks, which are more common worldwide, presents some integration challenges. Using multi-level converter systems is of the utmost importance at that stage. The novel non-isolated DC-DC MMC design proposed in this study provides a remarkable answer to the incorporation issues in power systems outlined above. The innovative non-isolated DC-DC MMC technology has been developed with inspiration from the investigations in [34, 35]. Fig. 8 shows the proposed innovative non-isolated DC-DC MMC design. The two-arm and one-arm architectural structures of the suggested non-isolated DC-DC MMC architecture are illustrated in Fig. 9a and Fig. 9b, respectively. The proposed non-isolated DC-DC MMC design's architectural framework and mathematical analysis have recently been described. The novel DC-DC MMC architecture suggested is non-isolated (transformerless) in structure.

The proposed converter topology benefits significantly from this method, which includes reduced volume, more appealing financing costs, fewer SM counts, lower weight, less power loss, etc. The construction of the suggested non-isolated converter is less complicated. This results in lower power loss and higher efficiency, which are crucial advantages, especially for energy conservation applications. Due to its more straightforward and less complicated construction, this converter is a cost-effective structure. Lower manufacturing expenses lead to lower overall system costs when isolating parts are absent. It also helps to save operating and maintenance expenses. This financial benefit becomes significant, particularly for large-scale power applications. This design results in a lightweight, non-isolated converter due to its more straightforward construction and fewer components. This functionality is quite beneficial, particularly for manufacturing and transportation procedures. The DC-DC MMC topology can provide excellent power density because it is designed in a non-isolated configuration. This approach enhances power transfer by enabling the converter structure to generate greater electrical power. The following sections of this research will examine how the proposed non-isolated DC-DC MMC architecture integrates with existing HVAC power systems.

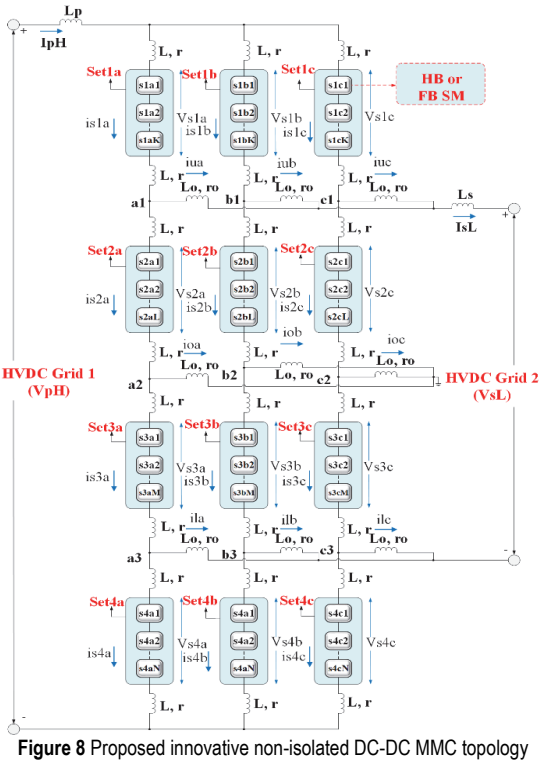

Figure 8 Proposed innovative non-isolated DC-DC MMC topology

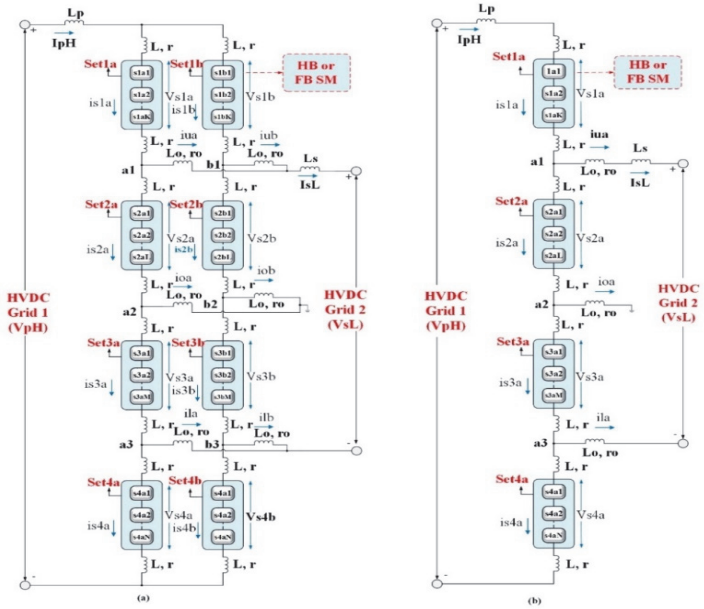

Figure 9 Proposed unique DC-DC MMC topology with 2-arm and 1-arm structures: (a) 2-arm structure; (b) 1-arm structure

3.1 The Proposed Non-isolated DC-DC MMC Design's Architectural Structure

Based on the fundamental concepts of the classical MMC approach, as shown in Fig. 8, the suggested non-isolated DC-DC MMC architecture is intended to accomplish DC-DC MMC conversion rather than DC-AC conversion. Similar to the traditional MMC architecture, the unique DC-DC MMC model that has been suggested has many arms, each including numerous SM clusters. The

recommended innovative DC-DC MMC design comprises three essential arms (arms a, b, and c). Four independent SM sets, each involving four HBSM structures (Set1a, Set2a, Set3a, and Set4a for arm-a), combine to form each arm. In this case, the primary rationale for utilizing the HBSM construction is its straightforward design, which strives to employ as few as conceivable power switches to minimize switching losses. The IGBT power switch based on semiconductors was chosen for the HBSM construction. These SM sets have been identified individually for each arm as top SM set (Set1a for arm-a), bottom SM set (Set4a for arm-a), middle top SM set (Set2a for arm-a), and middle bottom SM set (Set3a for arm-a).

There is one arm inductance (L, r) for each arm that occurs before and after the corresponding SM sets. The recommended DC-DC MMC design's secondary side positive terminal is formed by the branch arms that arise for each arm between the top and middle top SM sets (points $a1$, $b1$, and $c1$). These branch arms are connected sequentially through the arm filtering inductor (Lo, ro). The secondary side negative terminal of the recommended DC-DC MMC design has been formed like that of the system's output side positive terminal by a branch arm emerging between the bottom SM set and the middle bottom SM set (points $a3$, $b3$, and $c3$) for each arm and connected successively through the arm filtering inductor (Lo, ro). The centre ground branch arm of the proposed DC-DC MMC design is formed by a branch arm that emerges between the middle top SM set and the middle bottom SM set of each arm (points $a2$, $b2$, and $c2$). This branch arm is connected sequentially through the arm filtering inductor (Lo, ro), reminiscent of the formation of positive and negative secondary side terminals. In the proposed design, arm filtering inductors (Lo) make confident that the AC portion of the cycle is sufficiently diminished while arm inductors (L) among the SM sets soak up the short-term voltage variations arising from the switching process of the SMs in the cycle comprising the primary side of the architecture and the DC-DC MMC arms. According to the current levels flowing through the SM sets, the established voltage balancing and control system and the implementation of arm inductors (L) in the suggested novel DC-DC MMC architecture minimize any circulation currents in the arms at acceptable levels. The ohmic power losses related to L and Lo are represented by resistances r and ro, correspondingly. In the proposed DC-DC MMC design, Lp and Ls represent the filtering inductances of the design's primary and secondary side of the design, respectively.

3.2 The Proposed Non-isolated DC-DC MMC Design's Mathematical Model

Mathematical modelling is critical in adequately evaluating the recommended architectures in MMC technology. Several presumptions concerning the suggested MMC topologies must be established to conduct a more comprehensive mathematical analysis of the mathematical modelling under examination. This study's provided non-isolated DC-DC MMC architecture includes several hypothetical principles that validate the previously mentioned circumstance. Equivalent circuit models of MMC designs have been established based on these hypothetical assumptions. Fig. 10 demonstrates the circuit equivalent to the novel DC-DC MMC design that has been suggested. The 2-arm and 1-arm equivalent circuit designs of the suggested DC-DC MMC design are illustrated in Fig. 11a and Fig. 11b. A voltage source with a variable characteristic in this equivalent circuit structure represents each branch's SM groups. Voltage sources that alter over time consist of both DC and AC components. The mathematical counterparts of these DC and AC components are presented below.

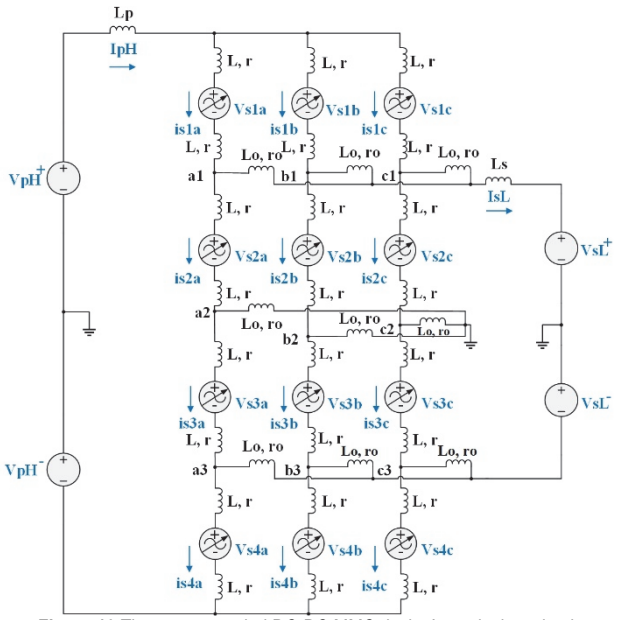

Figure 10 The recommended DC-DC MMC design's equivalent circuit

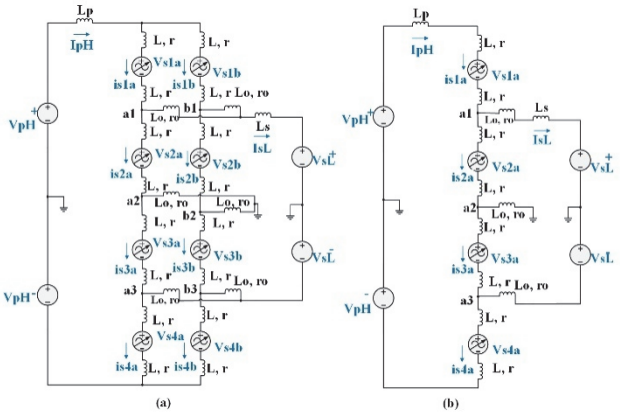

Figure 11 TheProposed novel DC-DC MMC design's equivalent circuits with 2-arm and 1-arm structures: (a) 2-arm equivalent circuit structure; (b) 1-arm equivalent circuit structure

According to the 1-arm equivalent circuit model (arm-a) of the suggested DC-DC MMC architecture, the mathematical computations provided in the following section have been carried out. Since similar mathematical analyses are valid for the other arms of the design (arms b and c), this study does not include mathematical evaluations for the two arms under consideration. The following mathematical parameters can be determined by applying the fundamental Kirchhoff Voltage Law and Kirchhoff Current Laws to the architecture of the 1-arm circuit illustrated in Fig. 11b. First and foremost, the following are the voltage equations for SM clusters.

$$v_{s1a} = \frac{v_{pH}}{2} - \frac{v_{sL}}{2} + 2L\frac{d}{dt}i_{s1a} + 2ri_{s1a} + \\ +V_{s1a,max}\,sin(\omega t) \quad (1)$$

$$v_{s2a} = \frac{v_{sL}}{2} + 2L\frac{\mathrm{d}}{\mathrm{d}t}i_{s2a} + 2ri_{s2a} + V_{s2a,\max}\sin(\omega t + \theta_1) \quad (2)$$

$$v_{s3a} = \frac{v_{sL}}{2} + 2L\frac{\mathrm{d}}{\mathrm{d}t}i_{s3a} + 2ri_{s3a} - V_{s3a,\max}\sin(\omega t + \theta_2) \quad (3)$$

$$v_{s4a} = \frac{v_{pH}}{2} - \frac{v_{sL}}{2} + 2L\frac{\mathrm{d}}{\mathrm{d}t}i_{s4a} + 2ri_{s4a} - \\ -V_{s4a,\max}\sin(\omega t + \theta_3) \quad (4)$$

$$i_{s1a} = I_{pH} = i_{s2a} + i_{s1a,uo} \quad (5)$$

$$i_{s2a} = i_{s3a} + i_{s1a,co} \quad (6)$$

$$i_{s4a} = i_{s3a} + i_{s1a,lo} \quad (7)$$

where $v_{s1a}, v_{s2a}, v_{s3a}$ and v_{s4a} denote the voltage expressions for the SM sets which are set1a, set2a, set3a and set4a in arm a, respectively. In keeping with the same logic $i_{s1a}, i_{s2a}, i_{s3a}$ and i_{s4a} represent the currents flowing through the SM sets which are set1*a*, set2*a*, set3*a* and set4*a* in arm *a*, correspondingly. The AC magnitude of the AC voltage of sets which are set1a, set2*a*, set3*a*, and set4*a* is represented by $V_{s1a,\max}, V_{s2a,\max}, V_{s3a,\max}$ and $V_{s4a,\max}$ respectively. θ_1, θ_2 and θ_3 are corresponding initial phase angles of SM sets voltage expression for arm-a. The angular frequency is represented by ω. The primary and secondary DC voltage levels of the suggested DC-DC MMC design are denoted by the V_{pH} and V_{SL}, correspondingly. Secondly, the current expressions of SM clusters are as follows.

$$i_{s1a} = I_{pH} + I_{s1a,\max}\sin(\omega t + \beta_1) \quad (8)$$

$$i_{s2a} = I_{pH} - \frac{V_{pH}}{V_{sL}}I_{pH} + I_{s2a,\max}\sin(\omega t + \beta_2) \quad (9)$$

$$i_{s2a} = I_{pH} - \frac{V_{pH}}{V_{sL}}I_{pH} + I_{s2a,\max}\sin(\omega t + \beta_2) \quad (10)$$

$$i_{s3a} = I_{pH} - \frac{V_{pH}}{V_{sL}}I_{pH} + I_{s3a,\max}\sin(\omega t + \beta_3) \quad (11)$$

$$i_{s4a} = I_{pH} - I_{s4a,\max}\sin(\omega t + \beta_4) \quad (12)$$

Examining the voltage and current expressions of the SM sets above reveals that each voltage and current parameter comprises two parts: DC and AC. The DC voltage components of the SM sets are represented by $v_{s1a,dc}, v_{s2a,dc}, v_{s3a,dc}$ and $v_{s4a,dc}$. $v_{s1a,ac}, v_{s2a,ac}, v_{s3a,ac}$ and $v_{s4a,ac}$, are the AC voltage components of sets of SM. Considering a comparable methodology, the AC components of the currents flowing through the SM sets are expressed by $i_{s1a,ac}, i_{s2a,ac}, i_{s3a,ac}$ and $i_{s4a,ac}$, while the DC components are expressed by $i_{s1a,dc}, i_{s2a,dc}, i_{s3a,dc}$ and $i_{s4a,dc}$. The AC magnitude of the AC voltage of sets which are set1a, set2a, set3a, and set4a is represented by $I_{s1a,\max}, I_{s2a,\max}, I_{s3a,\max}$ and $I_{s4a,\max}$ respectively. The phase angle of the currents flowing through the SM sets is represented by the letters $\beta_1, \beta_2, \beta_3$ and β_4. The following equation is the current flowing from point a2 through the grounding branch line. It is evident from Eq. (12) that the DC component is zero.

$$i_{s1a,co} = 21_{s1a,co,\max}\sin(\omega t + y) \quad (13)$$

The power expressions have been presented as follows, following the voltage and current expressions of the SM sets. In this case, branch inductances and resistors are disregarded to prevent an excessively involved mathematical examination and provide a more efficient power assessment.

$$p_{s1a} = \frac{V_{pH}}{2}I_{pH} - \frac{V_{sL}}{2}I_{pH} + \frac{V_{pH}}{2}I_{s1a,max}\,sin(\omega t + \beta_1) - \\ -\frac{V_{sL}}{2}I_{s1a,max}\,sin(\omega t + \beta_1) + \\ +\frac{V_{s1a,max}I_{s1a,max}}{2}cos(\beta_1) + V_{s1a,max}I_{pH}\,sin(\omega t) - \\ -\frac{V_{s1a,max}I_{s1a,max}}{2}\left[cos(2\omega t)cos(\beta_1) - sin(2\omega t)sin(\beta_1)\right] \quad (14)$$

where, p_{s1a} represents the power of the SM set st1a of arm-a. As seen in equation (13), the power expression consists of both DC and AC components, as in the case of voltage and current parameters, since it is inherently the product of the voltage falling on the relevant SM set and the current flowing through it. The power expressions of the set 2a set 3a, and set 4a SM sets of arm-a have been gathered with a similar approach and provided as p_{s2a}, p_{s3a}, and p_{s4a} correspondingly

$$p_{s2a} = \frac{V_{sL}}{2}I_{pH} - \frac{V_{pH}}{2}I_{pH} + \frac{V_{sL}}{2}I_{s2a,\max}\sin(\omega t + \beta_2) + \\ +\left[V_{s2a,\max}I_{pH} - V_{s2a,\max}I_{pH}\frac{V_{pH}}{V_{sL}}\right]\sin(\omega t + \theta_1) + \\ +\frac{V_{s2a,\max}I_{s2a,\max}}{2}\cos(\theta_1 - \beta_2) - \frac{V_{s2a,\max}I_{s2a,\max}}{2}\times \\ \times\left[\cos(2\omega t + 2\theta_1)\cos(\theta_1 - \beta_2) + \sin(2\omega t + 2\theta_1)\sin(\theta_1 - \beta_2)\right] \quad (15)$$

$$
\begin{aligned}
p_{s3a} &= \frac{V_{sL}}{2} I_{pH} - \frac{V_{pH}}{2} I_{pH} - \\
&- \frac{V_{sL}}{2} I_{s3a,\max} \sin(\omega t + \beta_3) - \\
&- V_{s3a,\max} I_{pH} + V_{s3a,\max} I_{pH} \frac{V_{pH}}{Vs_L} \sin(\omega t + \theta_2) + \\
&+ \frac{V_{s3a,\max} I_{s3a,\max}}{2} \cos(\theta_2 - \beta_3) - \frac{V_{s3a,\max} I_{s3a,\max}}{2} \times \\
&\times \left[\cos(2\omega t + 2\theta_2) \cos(\theta_2 - \beta_3) + \sin(2\omega t + 2\theta_2) \sin(\theta_2 - \beta_3) \right]
\end{aligned} \tag{16}
$$

$$
\begin{aligned}
p_{s4a} &= \frac{V_{pH}}{2} I_{pH} - \frac{V_{pH}}{2} I_{s4a,\max} \sin(\omega t + \beta_4) - \\
&- \frac{V_{sL}}{2} I_{pH} + \frac{V_{sL}}{2} I_{s4a,\max} \sin(\omega t + \beta_4) - \\
&- V_{s4a,\max} I_{pH} \sin(\omega t + \theta_3) + \frac{V_{s4a,\max} I_{s4a,\max}}{2} \cos(\beta_4 - \theta_3) - \\
&- \frac{V_{s4a,\max} I_{s4a,\max}}{2} \times \\
&\times \left[\cos(2\omega t + 2\theta_3) \cos(\theta_3 - \beta_4) + \sin(2\omega t + 2\theta_3) \sin(\theta_3 - \beta_4) \right]
\end{aligned} \tag{17}
$$

4 OPERATIONAL PRINCIPLE AND SIMULATION ANALYSIS OF THE DC-DC MMC TOPOLOGY

The suggested DC-DC MMC design's key objective is integrating HVAC and HVDC asynchronous networks with various voltage levels. That is the design's fundamental operation concept. Following the above mentioned desire, two approximately real-life asynchronous networks have been incorporated into the present investigation utilizing a simulation environment, as shown in Fig. 12. The system presented in this research has a primary end featuring a voltage level of 300 kV and a power of 210 MVA and a secondary end featuring a voltage level of 200 kV and a power of 190 MVA. The rectifier station that converts HVAC voltages into HVDC voltages is positioned on both the primary and secondary sides of the system. The fundamental objective of these rectifier stations is to ensure that the suggested system integrates with existing HVAC networks. The primary and secondary sides of the proposed DC-DC MMC system receive network voltages from rectifier stations, which convert HVAC voltage to HVDC voltage.

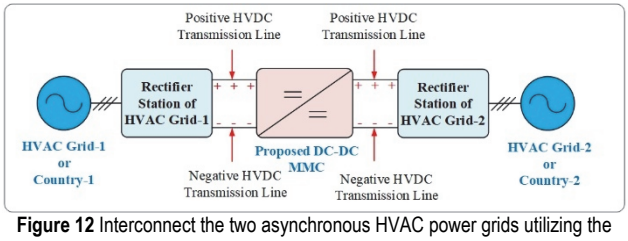

Figure 12 Interconnect the two asynchronous HVAC power grids utilizing the proposed DC-DC MMC design

The transformation and transfer processes under the control system's guidance are illustrated in Fig. 13. Fig. 13a shows the overall control system of the proposed innovative DC-DC MMC design. To achieve greater effectiveness in output power, the filtering system that filters the voltage and current values supplied from the networks to the DC-DC MMC architecture is depicted in Fig. 13b. Fig. 13c shows the Clarke transformation developed to determine the system characteristics needed for the suggested system and the circuit parameters required for an efficient DC voltage balancing system and effective power control. The sub-block diagram of the control system, which calculates the system parameters needed for the suggested topology, is displayed in Fig. 13d. Lastly, the power, current, and DC voltage control units in the proposed control system are illustrated in Fig. 9e. The design variables associated with the suggested system have been determined, which can be witnessed in the control system; the corresponding values have been supplied into the framework with the help of a filtering mechanism. Current, voltage, and power control mechanisms based on Proportional-Integral-Derivative Controllers (PID Controller), Clarke Transformation mechanism, and Phase Locked Loop structure have been utilized for this data transmission. In the stable αβ framework, the equilibrium two-phase orthogonal parts are obtained by applying the Clarke transformation to the equilibrium three-phase elements of HVAC Grid-1 and HVAC Grid-2 in the ABC referencing structure of the proposed topology.

Furthermore, the Clarke Transformation structure can generate the variables α, β, and zero by computing the Clarke transformation of the three-phase variables a, b, and c. The PLL module simulates a PLL closed-loop control framework that utilizes an inner frequency generator to monitor the frequency and phase of a sinusoidal wave. The controller modifies the inner generator frequency to maintain a zero-phase shift. The controller system's d-q transformation module utilizes the α and β variables obtained from Clarke Transformation to determine the quadratic axis (q) and direct axis (d) parameters. The signal computation section determines parameters under the values of the filter mechanism that the system controller implements. PID-based current, voltage, and power control units customize the required parameters to ensure the suggested DC-DC MMC system behaves reliably and steadily. A comprehensive efficiency analysis and loss model have been developed and applied to verify the proposed DC-DC topology's efficient bidirectional power transmission capability. The general control diagram illustrates how the parameters from the power controller, current, and DC voltage control units are assessed in this efficiency model, along with information from the unit that calculates the system parameters needed for the designed converter topology's efficient power transfer. Even though DC-DC converter systems have losses from capacitors, inductors, switching, power transmission, etc., the proposed design offers bidirectional power transfer with high efficiency and low losses in comparison to conventional MMC designs because it settles on minimal SM structures (HBSM), uses an efficient PWM technique, has a symmetrical and compact structure, and has an innovative control system developed.

The suggested DC-DC MMC is simulated in the simulation environment to demonstrate the system's effectiveness and functionality. Tab. 2 summarizes the parameters of the proposed DC-DC MMC topology, which is given in Fig. 8. Tab. 3 provides the control parameters of the control strategy incorporated into the suggested converter design. The following section presents the simulation outcomes obtained using the suggested design regarding the data in Tab. 2 and Tab. 3. In the present study, the individual Phase Disposition Pulse Width Modulation (PD-PWM) technology has been applied to

control power switching in SM architecture sets. IGBT power switches have been employed in the HBSM architecture of the suggested design, given that they have lower switching losses and a higher switching frequency and provide superior outcomes at higher voltage levels.

The simulated waveforms for the recommended research system have been illustrated in Fig. 14 to Fig. 24. Fig. 14 illustrates the primary side voltage (higher voltage level), primary side current, secondary side voltage (lower voltage level than the primary side), and secondary side current waveforms of the proposed DC-DC MMC design, respectively. The input and output voltage measurements of the suggested system are presented in Fig. 14's first and third waveforms. In contrast, Fig. 14's second and fourth waveforms display the input and output current measurements. The waveforms demonstrate a near-perfect DC characteristic for the voltage values, although harmonics cause some tolerable limited oscillates in the current values. These statistics, however, unambiguously demonstrate that the suggested system can transfer power and convert voltage from DC to DC. The voltage level of the primary side is 262 kV, while the secondary side is 184 kV, as demonstrated in Fig. 14. The corresponding primary and secondary side currents for the abovementioned voltage levels are 768 A and 1355 A, respectively. As provided in the mathematical examination in Section 3.2, voltage and current expressions consist of AC and DC characteristics. This situation causes some fluctuations, albeit at low levels, especially in the system's primary and secondary current waveforms. The findings above indicate that the DC-DC MMC design provides an equilibrium power transfer between two power networks. In other words, the functionality of the suggested novel DC-DC MMC and related control mechanisms can be demonstrated by the simulation results.

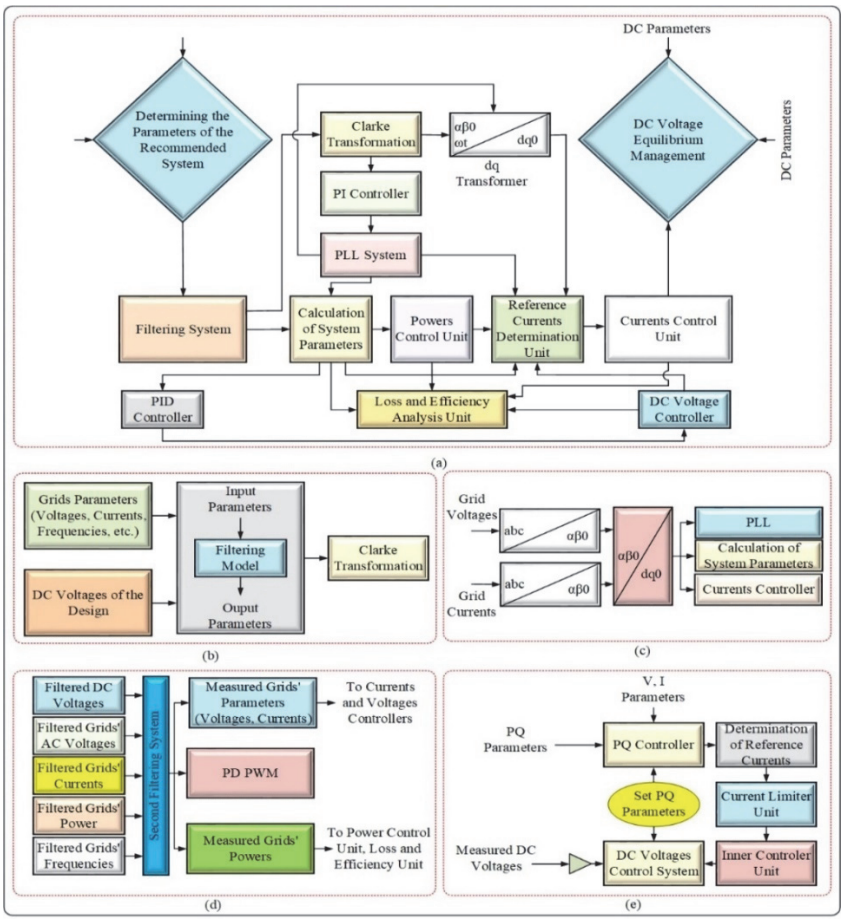

Figure 13 The Overall block diagrams of the proposed control system of unique DC-DC MMC topology: (a) general control system; (b) filtering system; (c) Clarke transformation; (d) calculation of the system parameters diagram; (e) powers, currents, and dc voltages of proposed controlling system for recommended topology.

Table 2 Parameters of the Simulated novel DC/DC MMC design

Parameters	Symbols	Values
HVDC Grid 1	VpH	262 kV
HVDC Grid 2	VsL	184 kV
Arm Filtering Inductor	Lo, ro[1]	20 mH
Arm Inductor	L, r[1]	3 mH
Number of HBSM per Sets	N	4
Number of Sets per Arm	M	4
HBSM Capacitor	VsC	10 mF
Switching Frequency	fswc	1000 Hz
Number of Arms, K	Arm-a, Arm-b Arm-c	3

[1] *The internal resistances of the inductors r and ro were neglected in the simulation analysis*

Table 3 Controllers' Parameters of the Simulated novel DC/DC MMC design

Parameters	Values
Proportional gain of power control, K_{pc}	4
Integral gain of power control, K_{ic}	4
Proportional gain of power regulator, K_{pr}	25
Integral gain of power regulator, K_{ir}	25
Proportional gain of current regulator, K_{pcr}	1
Integral gain of current regulator, K_{icr}	1
Proportional gain of DC voltage regulator, K_{pv}	3
Integral gain of DC voltage regulator, K_{iv}	50

The suggested DC-DC MMC topology's bidirectional power transfers are demonstrated in Fig. 15. The power

transfer waveform from the primary side to the secondary side is depicted in Fig. 15a, and the power transfer waveform from the secondary side to the primary side is illustrated in Fig. 15b. Fig. 15a and Fig. 15b show that the power transfer occurs 0.5 seconds after the system operates, with the control system executing a step activation. The primary and secondary power waveforms perfectly follow the reference signal. The power flow progressively exhibits behaviour consistent with the 0.9 p.u. reference signal. The power signals exhibit an exceptional reaction to abrupt changes in the system, such as voltage and power, occurring at 2 and 3.14 seconds. After the post, the power transfer stabilizes and proceeds after 3.14 seconds, following the reference signal. It is clear from examining the primary and secondary power transfer waveforms that the suggested converter design performs successfully during abrupt changes in the system's voltage and power in the suggested DC-DC MMC architecture. Outstanding rapid transient characteristics have been observed in the power transfers from the primary to the secondary side and from the secondary to the primary side in response to unexpected alterations in the system's parameters. For electrical networks to operate safely and sustainably, transient performance assessments of the systems are essential.

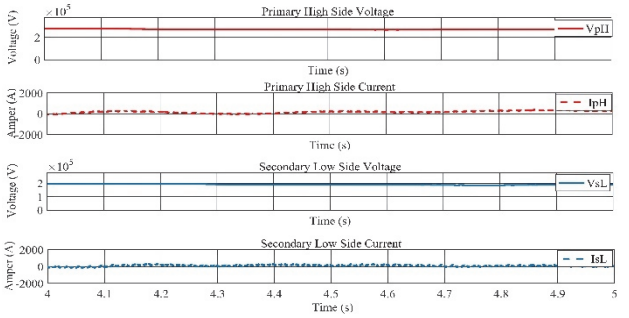

Figure 14 Voltage and current waveforms of the primary and secondary sides of the proposed DC-DC MMC topology

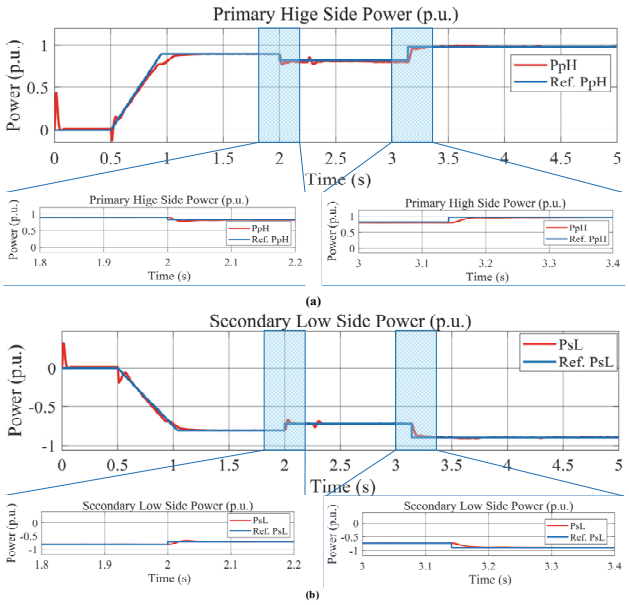

Figure 15 Power waveforms of the primary and secondary sides of the proposed DC-DC MMC topology: (a) the power waveform transferred from the primary side to the secondary side; (b) the power waveform transferred from the secondary side to the primary side

These studies support comprehending how the system functions, forecasting any issues, and establishing approaches for intervention whenever required. Consequently, it is visible from analysing the primary and secondary waveforms that the suggested DC-DC MMC architecture successfully facilitates power transfer between two asynchronous HVDC power grids.

The voltage across the four SM sets in system arm-a and the currents flowing through the appropriate SM sets are shown in Fig. 16 and Fig. 17. The novel configuration that has been suggested has three arms, each of which has four SM sets, as shown in Fig. 8. The PD-PWM approach, which operates based on reference signals with a 120 degree phase difference between each arm, has been employed for switching the power switches. The voltage and current waveforms of the SM set on arm-a are given to keep the research from getting excessively extensive. The waveforms for voltages and currents of the set1a and set2a SM sets have been demonstrated in Fig. 16, and the waveforms for the set3a and set4a SM sets have been displayed in Fig. 17.

Five distinguished voltage levels have been obtained since using four HBSMs in SM sets. As can be observed and predicted from the representation, the SM sets provide voltage values corresponding to different voltage levels, and the currents passing through them have the characteristics of a sinusoidal waveform. It is clear from examining the data produced by the pertinent voltage and current waveforms that the suggested architecture and associated control mechanisms operate admirably.

The waveforms of the capacitor voltages in the set1a SM set of the design's arm-a have been presented in Fig. 18. It is readily apparent that an efficient capacitor voltage balancing has been accomplished when glancing at the waveforms of the capacitor voltages in Fig. 18. In other words, it has been demonstrated that capacitor voltages are precisely regulated. The system's arm-a data illustrates that the innovative DC-DC MMC architecture that has been suggested successfully integrates two asynchronous power networks.

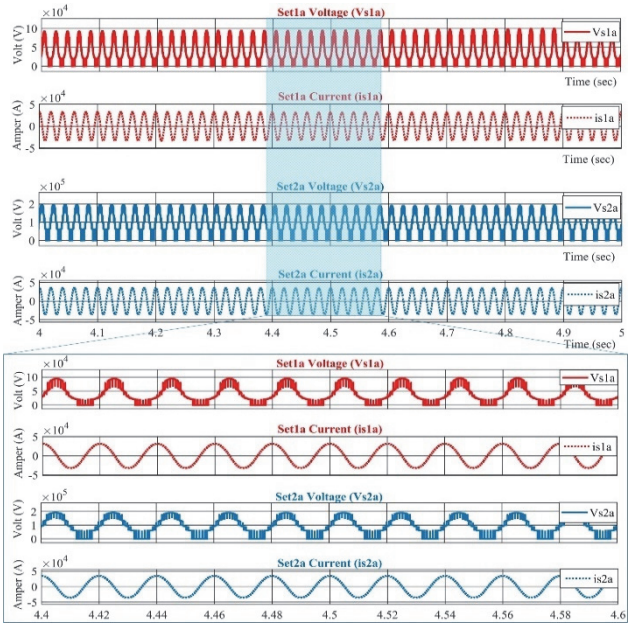

Figure 16 Voltages and currents of set 1a and set 2a

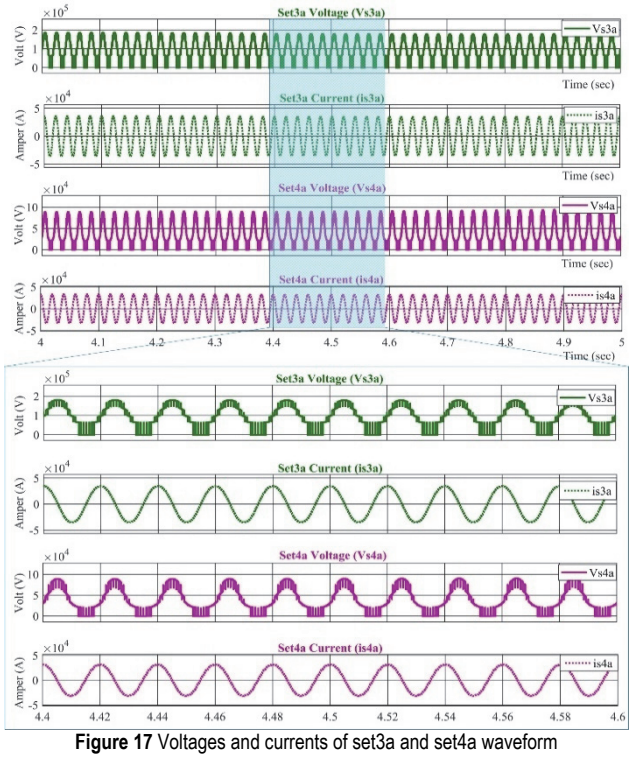

Figure 17 Voltages and currents of set3a and set4a waveform

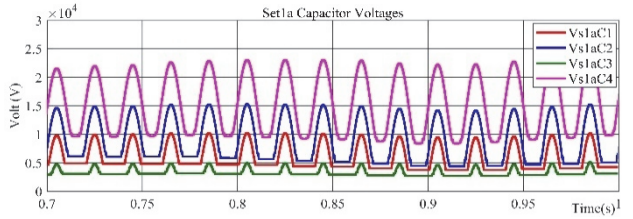

Figure 18 Set 1a capacitor voltages of arm-a.

The Fast Fourier Transform (FFT) analysis of the SM sets of the a-arm and the current and voltage waveforms of the primary and secondary sides of the suggested DC-DC MMC converter architecture have been depicted in Fig. 19 to Fig. 24. In cases where discrete impulses are transformed from the time domain to the frequency domain, the discrete Fourier transform is implemented and improved upon with FFT. The phases, structure of the frequencies and additional characteristics of the electrical signal are all revealed by FFT estimations. Electrical facilities' voltage, current, and power characteristics are supposed to follow a sine wave in power networks. Nevertheless, it is challenging for the current and waveforms in electrical networks to remain unadulterated sinusoidal owing to the expanding variety of modern industrial loads that are semiconductor-based and the power electronics-based converter systems located in many power systems presently. Therefore, the shape of a sine wave is no longer the sole pattern seen in the waveforms of power system network parameters. Harmonics are components of electrical power networks that deform waveforms of current and voltage parameters. It is expected that harmonic distortions will be observed to occur more frequently, particularly in power systems with substantial involvement from power electronics-based converter systems.

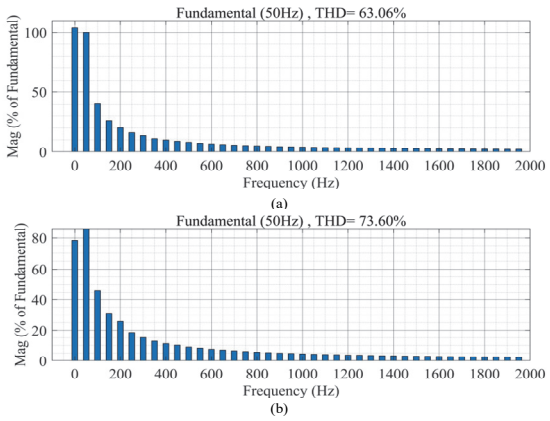

Figure 19 FFT analysis of primary waveforms: (a) Primary voltage FFT analysis; (b) Primary current FFT analysis

Nevertheless, thanks to their controllability and flexibility features, it is unavoidable that these types of structures will be employed in the modern power systems of the present day. In other words, these power electronics-based approaches are necessary for today's modern power systems to adapt optimally to modern load characteristics. Nonetheless, those mentioned above potential harmonic distortions can be minimized, providing that these designs, which are essentially expected to be utilized in present-day power systems, are developed in the most efficient and technologically advanced manner conceivable given their operational characteristics. These structures have superior control techniques that can mitigate harmonic distortions in addition to their optimal architecture. Considering the abovementioned information, the DC-DC MMC architecture presented in this research has been developed to offer ideal solutions for optimizing today's contemporary power systems. The highest-performing FFT analyses, which were carried out using the fundamental grid frequency (50 Hz) for this scenario, are shown in Fig. 19 to Fig. 24.

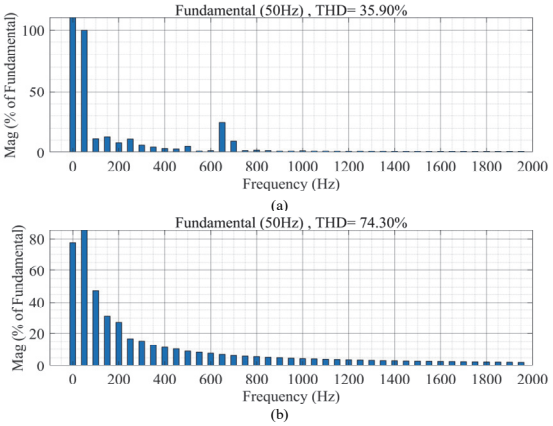

Figure 20 FFT analysis of secondary waveforms: (a) Secondary voltage FFT analysis; (b) Secondary current FFT analysis.

Fig. 19 presents the FFT analysis of the voltage and current waveforms of the proposed system's primary and secondary sides. In Fig. 19a and Fig. 20a, the Total Harmonic Distortion (THD) values corresponding to the voltage waveform of the primary and secondary sides are 63.06% and 35.90%, respectively. In Fig. 19b and Fig. 20b, the THD values of the primary and secondary currents waveforms were obtained as 73.60% and 74.30%. The FFT

analysis of the voltage waveforms occurring on the SM sets of the system's arm-a is illustrated in Fig. 21. While the THD value of the voltage falling on the set1a SM set in Figure 21a is 25.42%, the THD value of the voltage waveform of the se2a set in Fig. 21b has been calculated as 21.27%.

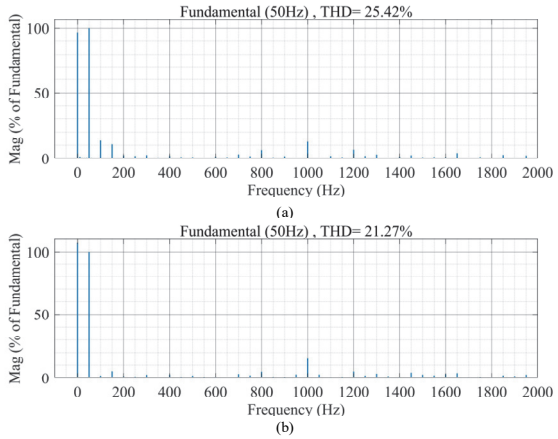

Figure 21 FFT analysis of arm-a voltages waveforms: (a) Set1a voltage FFT analysis; (b) Set2a voltage FFT analysis

Similarly, while the THD value of the voltage falling on the set3a SM set in Fig. 22a has been calculated as 21.73%, the THD value of the voltage waveform of the se4a set in Fig. 22b has been measured as 22.42%. Likewise, The FFT analysis of the current waveforms passing through the SM sets of the system's arm-a is illustrated in Fig. 23. While the THD value of the current passing through the set1a SM set in Fig. 23a is 3.05%, the THD value of the current waveform of the se2a set in Fig. 23b has been calculated as 2.97%. Similarly, while the THD value of the current passing through the set3a SM set in Fig. 24a has been calculated as 2.62%, the THD value of the current waveform of the se4a set in Fig. 24b has been measured as 3.25%. Considering the information above, it is unambiguous that the suggested DC-DC MMC structure integrates two asynchronous power networks while operating at maximal effectiveness, thanks to its innovative and modern construction. As can be provided, the THD statistics acquired by FFT analysis are at exceedingly acceptable ranges.

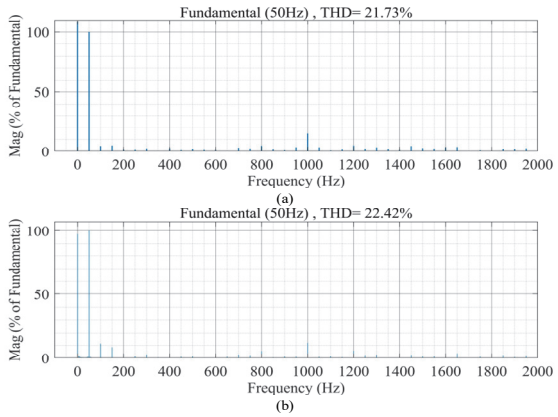

Figure 22 FFT analysis of arm-a voltages waveform: (a) Set3a voltage FFT analysis; (b) Set4a voltage FFT analysis.

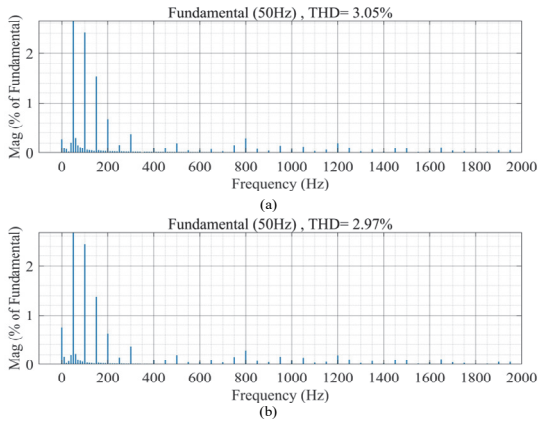

Figure 23 FFT analysis of arm-a currents waveform: (a) Set1a current FFT analysis; (b) Set2a current FFT analysis

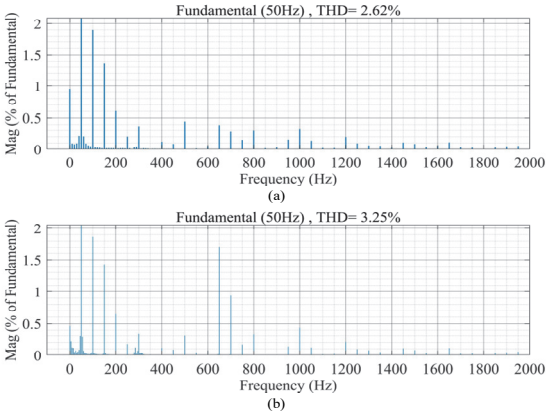

Figure 24 FFT analysis of arm-a currents waveform: (a) Set3a current FFT analysis; (b) Set4a current FFT analysis.

5 CONCLUSIONS

A revolutionary DC-DC MMC design is presented in this study to interconnect power networks with different voltage levels. Compared to the existing DC-DC MMC configurations in the literature, the proposed DC-DC MMC design provides many innovations, remarkable achievements, and enhancements. First, a novel topology has been designed for the proposed DC-DC MMC architecture. The novel architecture that has been suggested is crucial for integrating modern HVDC power systems with already existing HVAC power systems as well as interconnecting asynchronous revolutionary HVDC power grids. With its symmetrical and modular structure, the novel design that has been suggested can achieve optimum efficiency in bidirectional power transmission across power grids. The converter's volume, weight, cost, and power losses have been considerably reduced since the suggested topology has been developed thanks to a transformerless and compact methodology. An efficiency examination and loss model has been used to observe that the recommended DC-DC architecture successfully achieves bidirectional power transfer. Even though DC-DC converter systems have losses from capacitors, inductors, switching, power transmission, etc., the proposed design provides bidirectional power transfer with high efficiency and low losses in comparison to conventional MMC designs because it settles on minimal SM structures (HBSM), utilizes a successful PWM technique, has a symmetrical and compact structure, and

has an innovative control system. Whereas the majority of DC-DC MMC configurations in the literature offer solely DC-DC MMC analysis, the present investigation offers a significant analysis for both the integration of two asynchronous power systems that can occur in real life and the DC-DC MMC analysis of the recommended DC-DC MMC topology. According to the simulation data acquired, the control mechanism and architecture with such revolutionary flexibility, highly controllable capability, and unique characteristics have enabled the optimization of two asynchronous power networks to be accomplished effectively.

The design's functioning concept, mathematical analysis, simulation analysis, FFT analysis, and detailed architectural structure have all been skilfully conveyed. Although it is a power electronics-based design, it is clear that it exhibits effective performance according to the simulation results and FFT analysis. With its adaptable multiset construction, the suggested DC-DC MMC can scale up to very high-power levels, requiring no need for any transformer. Transformers at the primary and secondary ports, passive components, and sophisticated filtering mechanisms are all eliminated in non-isolated converter topologies such as the suggested DC-DC MMC architecture. In addition to achieving outstanding conversion rates utilizing reduced semiconductor devices and small-scale passive components, this drastically decreases the volume and size of converter topologies. The suggested transformerless converter design provides an opportunity to reduce switching losses and prevent the issues experienced while constructing transformers, thus minimizing system volume and expense. Undoubtedly, nonetheless, as compared to isolated DC-DC MMC topologies, the suggested DC-DC MMC architecture has shortcomings such as the absence of electrical isolation between the primary and secondary side of the systems, limitations in secondary voltage adaptation, difficulty customizing to more considerable power demands, greater secondary side voltage the presence of harmonics, and sophisticated controller processes. With its unique architectural structure and effective control mechanism, the suggested DC-DC MMC topology significantly reduces these shortcomings. The suggested converter exhibits several characteristics, including a straightforward circuit design, innovative structure, acceptable swift dynamic reaction, controllability, bidirectional power flow, and customizable operation, as observed from the simulation outcomes. Time-domain simulation analyses carried out in the simulation environment confirmed the assessment that has been presented. The simulation analysis results confirm the suggested non-isolated DC-DC MMC and associated customized control arrangement's viability, efficiency, and functionality.

5 REFERENCES

[1] Alatai, S., Salem, M., Ishak, D., Das, H. S., Alhuyi Nazari, M., Bughneda, A., & Kamarol, M. (2021). A Review on State-of-the-Art Power Converters: Bidirectional, Resonant, Multi-level Converters and Their Derivatives. *Applied Sciences*, *11*(21), 10172. https://doi.org/10.3390/app112110172

[2] Ang, T. Z., Salem, M., Kamarol, M., Das, H. S., Nazari, M. A., & Prabaharan, N. (2022). A comprehensive study of renewable energy sources: Classifications, challenges and suggestions. *Energy Strategy Reviews*, *43*, 100939. https://doi.org/10.1016/j.esr.2022.100939

[3] Razani, R. & Mohamed, Y. A. R. I. (2021). Analysis of the unsymmetrical operation of the DC/DC MMC considering the DC-Link impedance. *IEEE Transactions on Power Delivery*, *37*(3), 1723-1733. https://doi.org/10.1109/TPWRD.2021.3096498

[4] Chandio, R. H., Chachar, F. A., Soomro, J. B., Ansari, J. A., Munir, H. M., Zawbaa, H. M., & Kamel, S. (2023). Control and protection of MMC-based HVDC systems: A review. *Energy Reports*, *9*, 1571-1588. https://doi.org/10.1016/j.egyr.2022.12.056

[5] Liang, X. & Abbasipour, M. (2022). HVDC transmission and its potential application in remote communities: Current practice and future trend. *IEEE Transactions on Industry Applications*, *58*(2), 1706-1719. https://doi.org/10.1109/TIA.2022.3146117

[6] Yang, B., Liu, B., Zhou, H., Wang, J., Yao, W., Wu, S., & Ren, Y. (2022). A critical survey of technologies of large offshore wind farm integration: Summary, advances, and perspectives. *Protection and Control of Modern Power Systems*, *7*(2), 1-3. https://doi.org/10.1186/s41601-022-00239-w

[7] Ayobe, A. S. & Gupta, S. (2022). Comparative investigation on HVDC and HVAC for bulk power delivery. *Materials Today: Proceedings*, *48*, 958-964. https://doi.org/10.1016/j.matpr.2021.06.025

[8] Farkhani, J. S., Çelik, Ö., Ma, K., Bak, C. L., & Chen, Z. (2024). A comprehensive review of potential protection methods for VSC multi-terminal HVDC systems. *Renewable and Sustainable Energy Reviews*, *192*, 114280. https://doi.org/10.1016/j.rser.2024.114280

[9] Dey, S. & Bhattacharya, T. (2020). A transformerless DC-DC modular multi-level converter for hybrid interconnections in HVDC. *IEEE Transactions on Industrial Electronics*, *68*(7), 5527-5536. https://doi.org/10.1109/TIE.2020.2994889

[10] Erat, A. & Vural, A. M. (2022). DC/DC modular multi-level converters for HVDC interconnection: A comprehensive review. *International Transactions on Electrical Energy Systems*, *2022*(1), 2687243. https://doi.org/10.1155/2022/2687243

[11] Challa, R. V. K., Mikkili, S., & Bonthagorla, P. K. (2023). Modeling, controlling approaches, modulation schemes, and applications of modular multi-level converter. *Journal of Control, Automation and Electrical Systems*, *34*(1), 189-215. https://doi.org/10.1007/s40313-022-00953-8

[12] Bashir, S. B., Ismail, A. A. A., Elnady, A., Farag, M. M., Hamid, A. K., Bansal, R. C., & Abo-Khalil, A. G. (2023). Modular multi-level converter-based microgrid: A critical review. *IEEE Access*, *11*, 65569-65589. https://doi.org/10.1109/ACCESS.2023.3289829

[13] Marquardt, R. (2001).Stromrichterschaltungen mit verteilten energiespeichern. *German Patent DE10103031A1*, *24*, 40.

[14] Lesnicar, A. & Marquardt, R. (2003). An innovative modular multi-level converter topology suitable for a wide power range. *IEEE Bologna Power Tech Conference Proceedings, 3*, 6-pp). https://doi.org/10.1109/PTC.2003.1304403

[15] Li, R. & Xu, L. (2020). A unidirectional hybrid HVDC transmission system based on diode rectifier and full-bridge MMC. *IEEE Journal of Emerging and Selected Topics in Power Electronics*, *9*(6), 6974-6984. https://doi.org/10.1109/JESTPE.2020.3015342

[16] de Sousa, R. O., Cupertino, A. F., Morais, L. M. F., Pereira, H. A., & Teodorescu, R. (2023). Experimental validation and reliability analyses of minimum voltage control in modular multi-level converter-based statcom. *IEEE Transactions on Industrial Electronics*. https://doi.org/10.1109/TIE.2023.3303634

[17] Ansari, M. S., Shukla, A., & Bahirat, H. J. (2023). Analysis and design of MMC-based high-power DC–DC converter with trapezoidal modulation. *IEEE Transactions on Power Electronics*, *38*(6), 7256-7270. https://doi.org/10.1109/TPEL.2023.3249463

[18] He, R., Tian, K., & Ling, Z. (2023). Offline Equalization Control of Modular Multi-level Converter-Based Battery Energy Storage System. *IEEE Transactions on Industrial Electronics*. https://doi.org/10.1109/TIE.2023.3331145

[19] Goh, H. H., Sun, J., Liang, X., Zhang, D., Dai, W., Song, S., & Goh, K. C. (2024). Enhanced two-step nearest level control with enhanced power quality for electric ship system. *CSEE Journal of Power and Energy Systems*.

[20] Jia, G., Li, M., Shi, B., Yu, X., & Liu, X. (2023). A variable frequency injection method for modular multi-level converters in variable speed drives. *Energy Reports*, *9*, 939-947. https://doi.org/10.1016/j.egyr.2023.04.198

[21] Cheng, Q. & Chen, Y. (2021). A New Control Strategy of MMC-Based Active Power Filter Under Non-Ideal Conditions. *6th International Conference on Power and Renewable Energy (ICPRE)*, 22-27. https://doi.org/10.1109/ICPRE52634.2021.9635571

[22] Lyu, C., Lin, N., & Dinavahi, V. (2021). Device-level parallel-in-time simulation of mmc-based energy system for electric vehicles. *IEEE Transactions on Vehicular Technology*, *70*(6), 5669-5678. https://doi.org/10.1109/TVT.2021.3081534

[23] Haq, S., Biswas, S. P., Jahan, S., Islam, M. R., Rahman, M. A., Mahmud, M. P., & Kouzani, A. Z. (2021). An advanced PWM technique for MMC inverter based grid-connected photovoltaic systems. *IEEE Transactions on Applied Superconductivity*, *31*(8), 1-5. https://doi.org/10.1109/TASC.2021.3094439

[24] Zhao, S., Chen, Y., Cui, S., & Hu, J. (2022). Modular multi-level DC-DC converter with inherent bipolar operation capability for resilient bipolar MVDC grids. *CPSS Transactions on Power Electronics and Applications*, *7*(1), 37-48. https://doi.org/10.24295/CPSSTPEA.2022.00004

[25] Ashraf, M., Nazih, Y., Alsokhiry, F., Ahmed, K. H., Abdel-Khalik, A. S., & Al-Turki, Y. (2021). A new hybrid dual active bridge modular multi-level based DC-DC converter for HVDC networks. *IEEE Access*, *9*, 62055-62073. https://doi.org/10.1109/ACCESS.2021.3074543

[26] Qin, F., Hao, T., Gao, F., Xu, T., Niu, D., & Ma, Z. (2020, March). A multiport DC-DC modular multi-level converter for HVDC interconnection. In *2020 IEEE Applied Power Electronics Conference and Exposition (APEC)*, 520-524. https://doi.org/10.1109/APEC39645.2020.9124277

[27] Sarkar, S. & Das, A. (2022). An isolated single input-multiple output DC-DC modular multi-level converter for fast electric vehicle charging. *IEEE Journal of Emerging and Selected Topics in Industrial Electronics*, *4*(1), 178-187. https://doi.org/10.1109/JESTIE.2022.3221006

[28] Zhao, S., Chen, Y., Cui, S., Mortimer, B. J., & De Doncker, R. W. (2020). Three-port bidirectional operation scheme of modular-multilevel DC–DC converters interconnecting MVDC and LVDC grids. *IEEE Transactions on Power Electronics*, *36*(7), 7342-7348. https://doi.org/10.1109/TPEL.2020.3041721

[29] Mehrabankhomartash, M., Yin, S., Kandula, R. P., Divan, D., & Saeedifard, M. (2023). Analysis and Design Guidelines of the Isolated Modular Multi-level DC-DC Converter With the Impact of Magnetizing Inductance. *IEEE Transactions on Industrial Electronics*, *70*(12), 11911-11922. https://doi.org/10.1109/TIE.2023.3236111

[30] Elserougi, A., Abdelsalam, I., & Massoud, A. (2023). A hybrid half-bridge submodule-based DC-DC modular multi-level converter with a single bidirectional high-voltage valve. *IET Generation, Transmission & Distribution*, *17*(18), 4146-4160. https://doi.org/10.1049/gtd2.12974

[31] Ansari, M. S., Shukla, A., & Bahirat, H. J. (2023). A Novel Hybrid Multi-level DC-DC Converter Employing Trapezoidal Modulation. *IEEE Transactions on Power Electronics*, *38*(10), 12679-12691. https://doi.org/10.1109/TPEL.2023.3288984

[32] Ning, G., Dai, B., Su, M., Shu, L., & Xiong, W. (2024). Interleaved Buck-Integrated Modular Multi-level DC Transformer with Wide Voltage Range for DC Distribution Grids. *IEEE Transactions on Power Electronics*. https://doi.org/10.1109/TPEL.2024.3377466

[33] Wang, Y., Aksoz, A., Geury, T., Ozturk, S. B., Kivanc, O. C., & Hegazy, O. (2020). A Review of Modular Multi-level Converters for Stationary Applications. *Applied Sciences*, *10*(21), 7719. https://doi.org/10.3390/app10217719

[34] Acero, D. G., Cheah-Mane, M., Páez, J. D., Morel, F., Gomis-Bellmunt, O., & Dworakowski, P. (2021). Dc-MMC for the interconnection of HVDC grids with different line topologies. *IEEE Transactions on Power Delivery*, *37*(3), 1692-1703. https://doi.org/10.1109/TPWRD.2021.3095966

[35] Razani, R. & Mohamed, Y. A. R. I. (2022). Model predictive control of non-isolated DC/DC modular multi-level converter improving the dynamic response. *IEEE Open Journal of Power Electronics*, *3*, 303-316. https://doi.org/10.1109/OJPEL.2022.3176833

Contact information:

Abdurrahim ERAT
(Corresponding author)
Electrical and Electronics Engineering Department,
Gaziantep University,
27310 Gaziantep, Turkey
E-mail: a.rahim_erat@sirnak.edu.tr

Ahmet Mete VURAL, PhD, Full Prof
Electrical and Electronics Engineering Department,
Gaziantep University,
27310 Gaziantep, Turkey
E-mail: mvural@gantep.edu.tr